

Effect of the Al content on the optical phonon spectrum in $\text{Mg}_{1-x}\text{Al}_x\text{B}_2$

P. Postorino,¹ A. Congeduti,¹ P. Dore,¹ A. Nucara,¹ A. Bianconi,¹ D. Di Castro,¹ S. De Negri,² and A. Saccone²

¹*Istituto Nazionale di Fisica della Materia and Dipartimento di Fisica, Universita' di Roma "La Sapienza," Piazzale A. Moro 2, 00185 Roma, Italy*

²*Dipartimento di Chimica e Chimica Industriale, Universita' di Genova, Via Dodecanneso 31, 16146 Genova, Italy*

(Received 6 July 2001; published 19 December 2001)

Raman and infrared absorption spectra of $\text{Mg}_{1-x}\text{Al}_x\text{B}_2$ have been collected for $0 \leq x \leq 0.5$ in the frequency range of the phonon spectrum. The data show a remarkable dependence on the Al content. Raman spectra have been carefully analyzed and the x dependence of the peak frequency, the width and the intensity of the phonon modes have been obtained. The results allow us to distinguish between two regimes in the low and high Al content regions. In particular the onset of the high Al content phase evidenced in previous structural studies is marked by new spectral components at high frequencies. Finally a connection between the whole of our results and the suppression of the superconducting phase at high Al content is established.

DOI: 10.1103/PhysRevB.65.020507

PACS number(s): 74.70.-b, 74.25.Kc, 78.30.-j

The recent discovery¹ of superconductivity below 39 K in MgB_2 has stimulated a great deal of effort among the scientific community and a large number of theoretical and experimental papers have been published within a few months. The debate on the origin of this unexpected superconductivity is still open, although an increasing number of both experimental²⁻⁴ and theoretical⁵⁻⁷ works indicate that MgB_2 is a BCS-like system. Owing to the simple hexagonal structure (space group P_6mmm), four zone-center optical modes are predicted for MgB_2 : a silent B_{1g} mode, the E_{2g} Raman mode, and the infrared active E_{2u} and A_{2u} modes. While the doubly degenerate E_{2u} and E_{2g} modes are ascribed to in-plane stretching modes of the boron atoms, both nondegenerate A_{2u} and B_{1g} modes involve vibrations along the perpendicular direction (c axis). In the BCS framework, the obvious relevant interaction in the superconducting transition is the electron-phonon (e-ph) coupling and many theoretical works agree in identifying the E_{2g} as the mainly involved mode.⁵⁻⁷ The quite large and asymmetric band around 600 cm^{-1} which dominates the Raman spectrum of MgB_2 has been ascribed to the E_{2g} mode and its anomalous width interpreted as a signature of the e-ph coupling.⁸⁻¹²

Up to now, no other isostructural boride (XB_2) shows the peculiar high-temperature superconductivity of MgB_2 and in particular no superconducting phase has been found in AlB_2 . Several studies carried out on $\text{Mg}_{1-x}\text{Al}_x\text{B}_2$ compounds have indeed shown that the superconducting transition temperature T_c is progressively reduced for increasing x and vanishes for $x > 0.50$.¹³⁻¹⁵ The Al content induces also remarkable structural modifications. Different x-ray diffraction measurements have indeed shown the occurrence of two distinct structural phases in the low (LC, $0 < x < x_1$) and in the high (HC, $x > x_2$) Al content regions. The border concentrations for the two phases are not yet well defined, since the values reported for x_1 and x_2 ranges from 0.09 to 0.13 and from 0.20 to 0.33, respectively.^{13,15,16} The nature of the structural phase in the intermediate x region ($x_1 < x < x_2$) is still under debate; both a two phase region¹³ and a disordered phase¹⁶ have indeed been proposed.

In order to achieve a deeper understanding of the effects of the Al content, we have studied the evolution of the phonon spectrum of $\text{Mg}_{1-x}\text{Al}_x\text{B}_2$ in the $0 \leq x \leq 0.5$ range by means of both Raman and infrared spectroscopy. Polycrystalline samples of $\text{Mg}_{1-x}\text{Al}_x\text{B}_2$ have been synthesized at high temperature by direct reaction of the elements in a tantalum crucible under argon atmosphere. The samples have been characterized by x-ray diffraction and the x dependence of T_c has been carefully determined.^{14,16}

The Raman spectra were measured in back-scattering geometry, using a micro-Raman spectrometer with a charge-coupled device camera and an adjustable notch filter. The sample was excited by the 632.8 nm line of a 16 mW He-Ne Laser. The confocal microscope was equipped with a 20 \times magnification objective which gives a laser spot about $10 \mu\text{m}^2$ wide at the sample surface. The explored Raman shift ranges between 200 and 1100 cm^{-1} , the low-frequency limit being due to the notch filter cutoff. The relative intensities of the observed spectral features were slightly different from point to point, depending on the random orientation of the microcrystals. For each sample, Raman spectra were thus collected from different points and then averaged.

As shown in Fig. 1(a), the spectrum of the MgB_2 sample is dominated by a band centered around 600 cm^{-1} (ν_2), in agreement with previous Raman experiments.⁸⁻¹² Although the origin of this band is still questioned,^{11,12} it is generally assigned to the only Raman-active mode E_{2g} , to which theoretical predictions attribute a peak frequency^{6,7,9,12,17,18} ranging from 470 to 660 cm^{-1} . A close inspection of Fig. 1(a) reveals also two weak shoulders around 400 (ν_1) and 750 cm^{-1} (ν_3) on the high- and low-frequency side of the ν_2 band. Also in previous Raman experiments,^{10,12} beside the dominant ν_2 band, other spectral contributions have been observed and ascribed to peaks in the phonon density of states,¹⁹ forbidden in the framework of the factor group analysis. As a matter of fact, in disordered or defective system, the momentum selection rules can be violated, and the Raman (or infrared absorption) spectrum can partially reflect the phonon density of states.

The MgB_2 spectrum was fitted by a function successfully used in modeling broad Raman spectra in strongly correlated systems:^{20,21}

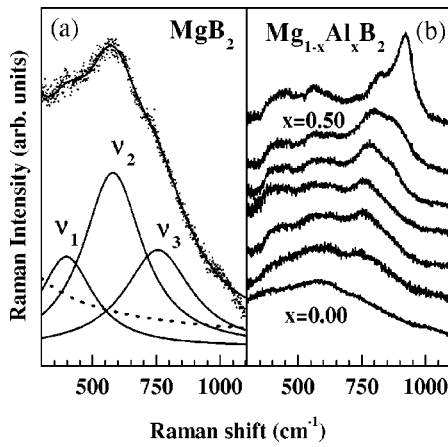


FIG. 1. (a) Raman spectrum of MgB_2 and the best fit curve from Eq. (1) (solid line). The three phonon contributions (solid lines) and the $\nu=0$ background (dashed line) are also shown separately. (b) Raman spectra of $\text{Mg}_{1-x}\text{Al}_x\text{B}_2$ at $x=0, 0.08, 0.17, 0.25, 0.33, 0.41, 0.50$ after background subtraction. The spectra are shifted vertically for clarity.

$$S(\nu) = [1 + n(\nu)] \left[\frac{A\nu\Gamma}{\nu^2 + \Gamma^2} + \sum_{i=1}^N \frac{A_i\nu\Gamma_i}{(\nu^2 - \nu_i^2)^2 + \nu^2\Gamma_i^2} \right]. \quad (1)$$

The first term represents a low-frequency contribution describing the wide and unstructured electronic background, which is a common feature of strongly correlated systems such as manganites and cuprates.⁸ The second term is a combination of damped harmonic oscillators describing N phonon peaks, where ν_i , A_i , and Γ_i are peak frequency, amplitude, and linewidth, respectively. The quantity $n(\nu)$ is the Bose-Einstein thermal population factor. In Fig. 1(a) we also report the best fit spectrum, the tail of the electronic background, and the ν_1 , ν_2 , and ν_3 components ($\nu_1=415 \pm 20 \text{ cm}^{-1}$, $\nu_2=605 \pm 10 \text{ cm}^{-1}$, and $\nu_3=780 \pm 30 \text{ cm}^{-1}$). We point out that these peak frequencies are in a quite good agreement with those observed in the phonon density of states derived from neutron scattering experiments, where different optical contributions have been found around 430, 620, 710 and 780 cm^{-1} .¹⁹

The spectra of the doped $\text{Mg}_{1-x}\text{Al}_x\text{B}_2$ samples are also well reproduced by using Eq. (1) if, for $x > 0.10$, the phonon number N is increased from 3 to 4. In Fig. 1(b) we report the Raman spectra for different Al content after background subtraction. The ν_3 contribution which is just a weak shoulder in the pure sample, becomes well detectable in the $x=0.08$ spectrum. Both its intensity and peak frequency increase on further increasing x . For $x > 0.10$, a new component (ν_4) appears around 850 cm^{-1} and, for $x > 0.30$, the ν_3 and ν_4 peaks become the dominant contributions to the Raman spectrum.

Infrared absorption measurements on $\text{Mg}_{1-x}\text{Al}_x\text{B}_2$ were performed above 400 cm^{-1} by using a Bomem MB100 interferometer operating with a resolution of 10 cm^{-1} . Following a standard procedure,²² we measured the optical density $O_d(\nu) = \ln[I_o(\nu)/I(\nu)]$, where $I_o(\nu)$ is the infrared signal transmitted by a pure CsI pellet and $I(\nu)$ that transmitted by

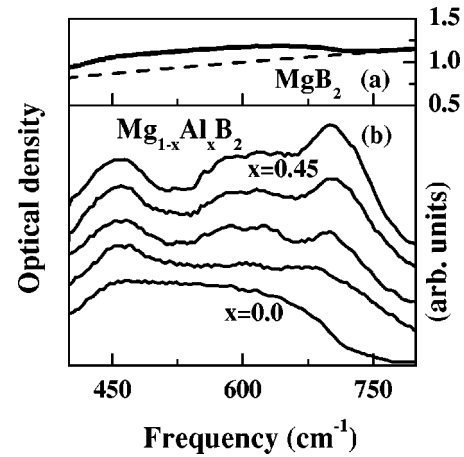


FIG. 2. (a) Far infrared optical density of MgB_2 . The background is also shown (dashed line). (b) Optical densities of $\text{Mg}_{1-x}\text{Al}_x\text{B}_2$ at $x=0, 0.17, 0.33, 0.41, 0.45$ after background subtraction. The spectra are shifted vertically for clarity.

the sample powder dispersed in a CsI pellet. The far infrared $O_d(\nu)$ of the measured $\text{Mg}_{1-x}\text{Al}_x\text{B}_2$ samples are characterized by a weak phonon spectrum, owing to screening effects from free charges, superimposed to a broad and intense background as shown in Fig. 2(a) for the MgB_2 case. These phenomena, already observed when the above procedure is employed for measuring metallic powder samples,²³ prevent to achieve reliable fits of the experimental data. However, once the background is subtracted, a clear picture of the effect of the Al content on the far infrared spectrum of $\text{Mg}_{1-x}\text{Al}_x\text{B}_2$ is obtained, as shown in Fig. 2(b). The MgB_2 spectrum [see Fig. 2(b)] can be described by considering a broad peak centered around 460 cm^{-1} , accompanied by a very broad band around 600 cm^{-1} . Since the infrared-active E_{1u} and A_{2u} phonons are predicted^{6,7,9,12,17,18} around 330 and 400 cm^{-1} , the two observed bands can be ascribed to infrared forbidden peaks in the phonon density of states,¹⁹ as previously discussed. It is worth to notice that the present MgB_2 spectrum is in a qualitative agreement with a previous measurement, where a broad peak centered around 480 cm^{-1} is accompanied by further components at higher frequencies.²⁴ The spectra of $\text{Mg}_{1-x}\text{Al}_x\text{B}_2$ [see Fig. 2(b)] clearly show the effect of Al content. While the 460 cm^{-1} band becomes more evident with increasing the Al content, a new absorption peak appears around 700 cm^{-1} for $x > 0.17$ and strongly increases on further increasing the Al content. Both Raman and infrared spectra thus give evidence that the Al content induces substantial modifications of the MgB_2 optical properties and the appearance of new high-frequency contributions suggests the occurrence of remarkable structural changes at high Al content.

A careful analysis of the Raman spectra, and in particular of the x -dependence the best-fit values ν_i and Γ_i , provides a more detailed and quantitative description of the effect of the Al content. While the ν_1 peak does not significantly vary with the Al content, its peak frequency and width being almost constant in the $0-0.5$ x range ($\nu_1 \approx 415 \text{ cm}^{-1}$, $\Gamma_1 \approx 100 \text{ cm}^{-1}$), more relevant information can be extracted from the peaks at higher frequencies. The x -dependence of

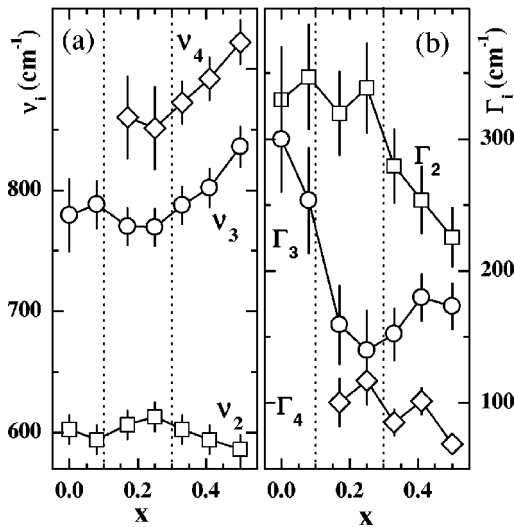


FIG. 3. Best fit values of ν_i (a) and Γ_i (b) ($i=2,3,4$) as function of x from the analysis of the Raman spectra. Vertical dashed lines indicate the $x=0.10$ and $x=0.30$ values.

the ν_i and Γ_i best-fit values ($i=2,3,4$) shown in Fig. 3 allow us to discriminate between a low and an high Al content regime. This observation is in agreement with the occurrence of the previously discussed LC and HC structural phases. Consistently with the different x_1 and x_2 border values reported in literature,^{13,15,16} the two vertical lines at $x=0.10$ and at $x=0.30$ in Fig. 3 qualitatively identify the extension of the two structural phases. In the different x -regions a quite different behavior can be observed. As shown in Fig. 3(a), ν_2 and ν_3 are nearly constant in the LC phase. The onset of the HC phase in the intermediate x -region is marked by the appearance of the new spectral feature (ν_4). When the system enters the pure HC phase, both ν_3 and ν_4 strongly increase with x , while ν_2 remains nearly constant. At the moment, our results do not allow a complete and reliable assignment of the observed Raman lines, possible through a polarization analysis of Raman spectra from high-quality single crystals. We just note that the weak x dependence of the ν_2 mode is consistent with its assignment to the in-plane E_{2g} stretching mode of the boron atoms, since the a (in-plane) lattice parameter does not significantly vary with x .^{13,15,16}

As far as the phonon widths Γ_i are concerned, the LC phase is characterized by quite large values for Γ_2 and Γ_3 [see Fig. 3(b)]. In the intermediate x -region a fast drop of Γ_3 occurs, while Γ_2 strongly decreases only on entering the HC phase. Since the phonon width is usually considered as a marker of the extent of the e-ph coupling, the overall narrowing of the high-frequency peaks suggests a generalized reduction of this coupling with increasing the Al content. In particular, given that ν_2 is considered the most relevant phonon in the superconducting transition, the strong decrease of Γ_2 could be related to the observed steepening of the x dependence of T_c on entering the HC phase shown in Fig. 4(a).¹⁶

Finally, although a comparison among the absolute intensities of different spectra may be questionable, a comparative analysis of the peak integrated intensities I_i can be safely

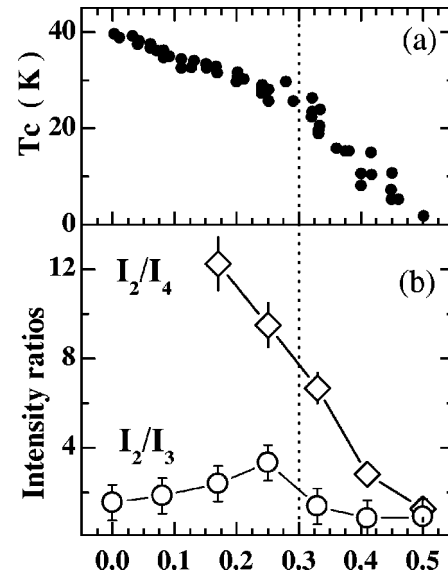


FIG. 4. (a) T_c as a function of x from Ref. 16. (b) I_2/I_3 and I_2/I_4 intensity ratios (see text) as a function of x from the analysis of Raman spectra. The vertical dashed line indicate the $x=0.30$ value.

performed. In Fig. 4(b) the I_2/I_3 and I_2/I_4 values as a function of x are reported. It is well evident that both ratios decrease for $x > 0.30$, albeit I_2/I_4 is much steeper than I_2/I_3 . This result reflects the progressive transformation of the structure from the LC to the HC phase. As a matter of fact, the importance of the ν_2 mode with respect to the ν_3 and in particular to the ν_4 mode (peculiar of the HC region) decreases with increasing x in the HC phase. The comparison between the x dependence of T_c [Fig. 4(a)] and of the intensity ratios [Fig. 4(b)] strongly suggests a correlation between superconductivity and phonon structures of $\text{Mg}_{1-x}\text{Al}_x\text{B}_2$. The increase of importance of the ν_3 and ν_4 with respect to the ν_2 phonon, associated with the structural phase transition, seems to be strongly related to the decrease of T_c with increasing x .

In conclusion, the present Raman and infrared measurements of $\text{Mg}_{1-x}\text{Al}_x\text{B}_2$ show a strong dependence of the phonon spectrum on the Al content in the 0–0.50 x range. A careful analysis of the Raman peaks shows the presence of at least two distinct regimes in the low and in the high Al content region. This result is in agreement with the occurrence of the HC and LC structural phases observed by x-ray diffraction measurements.^{13,15,16} Although our data do not allow for a definite assignment of the observed Raman peaks, the x dependence of the ν_2 phonon is consistent with its assignment to the E_{2g} mode. The narrowing of the phonon widths with increasing the Al content suggests a significant reduction of the e-ph coupling which, in a BCS scenario, causes the observed decrease of T_c . In particular, both a remarkable drop of Γ_2 and a steepening of the T_c decrease occur on increasing x in the HC phase. Finally, the suppression of superconductivity in the HC regime seems to be directly related to the decrease of the importance of the ν_2 with respect to the ν_3 and ν_4 modes which dominate the high Al content phase.

- ¹J. Nagamatsu, N. Nakagawa, T. Muranaka, Y. Zenitani, and J. Akimitsu, *Nature (London)* **410**, 63 (2001).
- ²S.L. Bud'ko, G. Lapertot, C. Petrovic, C.E. Cunningham, N. Anderson, and P.C. Canfield, *Phys. Rev. Lett.* **86**, 1877 (2001).
- ³T. Takahashi, T. Sato, S. Souma, T. Muranaka, and J. Akimitsu, *Phys. Rev. Lett.* **86**, 4915 (2001).
- ⁴G. Rubio-Bollinger, H. Suderov, and S. Vieira, *Phys. Rev. Lett.* **86**, 5582 (2001).
- ⁵J.M. An and W.E. Pickett, *Phys. Rev. Lett.* **86**, 4366 (2001).
- ⁶J. Kortus, I.I. Mazin, K.D. Belashchenko, V.P. Antropov, and L.L. Boyer, *Phys. Rev. Lett.* **86**, 4656 (2001).
- ⁷Y. Kong, O.V. Dolgov, O. Jepsen, and O.K. Andersen, *Phys. Rev. B* **64**, 020501(R) (2001).
- ⁸A.F. Goncharov, V.V. Struzhkin, E. Gregoryanz, J. Hu, R.J. Hemley, H. Mao, G. Lapertot, S.L. Bud'ko, and P.C. Canfield, *Phys. Rev. B* **64**, 100509(R) (2001); A.F. Goncharov, V.V. Struzhkin, E. Gregoryanz, H. Mao, R.J. Hemley, G. Lapertot, S.L. Bud'ko, P.C. Canfield, and I.I. Mazin, *cond-mat/0106278* (unpublished).
- ⁹K.P. Bohnen, R. Heid, and B. Renker, *Phys. Rev. Lett.* **86**, 5771 (2001).
- ¹⁰J. Hlinka, I. Gregora, J. Pokorny, L. Plecenik, P. Kus, L. Satrapinsky, and S. Benacka, *Phys. Rev. B* **64**, 140503 (2001).
- ¹¹X.K. Chen, M.J. Kostantinovic, J.C. Irwin, D.D. Lawrie, and J.P. Franck, *Phys. Rev. Lett.* **87**, 157002 (2001).
- ¹²K. Kunc, I. Loa, K. Syassen, R.K. Kremer, and K. Ahn, *cond-mat/0105402* (unpublished).
- ¹³J.S. Slusky, N. Rogado, K.A. Regan, M.A. Hayward, P. Khalifah, T. He, K. Inumaru, S.M. Loureiro, M.K. Haas, H.W. Zandbergen, and R.J. Cava, *Nature (London)* **410**, 342 (2001).
- ¹⁴A. Bianconi, D. Di Castro, S. Agrestini, G. Campi, N.L. Saini, A. Saccone, S. De Negri, and M. Giovannini, *J. Phys.: Condens. Matter* **13**, 7383 (2001).
- ¹⁵J.Y. Xiang, D.N. Zheng, J.Q. Li, L. Li, P.L. Lang, H. Chen, C. Dong, G.C. Che, Z.A. Ren, H.H. Qi, H.Y. Tian, Y.M. Ni, and Z.X. Zhao, *cond-mat/0104366* (unpublished).
- ¹⁶A. Bianconi, D. Di Castro, S. Agrestini, G. Zangari, N.L. Saini, A. Saccone, S. De Negri, M. Giovannini, G. Profeta, A. Continenza, G. Satta, S. Massidda, A. Cassetta, A. Pifferi, and M. Colapietro (unpublished).
- ¹⁷G. Satta, G. Profeta, F. Bernardini, A. Continenza, and S. Massidda, *Phys. Rev. B* **64**, 104507 (2001).
- ¹⁸T. Yildirim, O. Gulseren, J.W. Lynn, C.M. Brown, T.J. Udovic, H.Z. Qing, N. Rogado, K.A. Regan, M.A. Hayward, J.S. Slusky, T. He, M.K. Haas, P. Khalifah, K. Inumaru, and R.J. Cava, *Phys. Rev. Lett.* **87**, 037001 (2001).
- ¹⁹R. Osborn, E.A. Goremychkin, A.I. Kolesnikov, and D.G. Hinks, *Phys. Rev. Lett.* **87**, 017005 (2001).
- ²⁰S. Yoon, H.L. Liu, G. Schollerer, S.L. Cooper, P.D. Han, D.A. Payne, S.W. Cheong, and Z. Fisk, *Phys. Rev. B* **58**, 2795 (1998).
- ²¹A. Congeduti, P. Postorino, E. Caramagno, M. Nardone, A. Kumar, and D.D. Sarma, *Phys. Rev. Lett.* **86**, 1251 (2001).
- ²²P. Calvani, G. De Marzi, P. Dore, S. Lupi, P. Maselli, F. D'Amore, S. Gagliardi, and S.W. Cheong, *Phys. Rev. Lett.* **81**, 4504 (1998).
- ²³P. Dore, G. De Marzi, R. Bertini, A. Nucara, P. Calvani, and M. Ferretti, *Physica C* **350**, 55 (2001).
- ²⁴C.S. Sundar, A. Bharathi, M. Premila, T.N. Sairam, S. Kalavathi, G.L.N. Reddy, V.S. Sastry, Y. Hariharan, and T.S. Radhakrishnan, *cond-mat/0104354* (unpublished).